

Fe<sub>3</sub>O<sub>4</sub> nanoparticles investigated by vibrating sample magnetometry and muon spin relaxation

Charlotte Read

A senior thesis submitted to the faculty of

Brigham Young University

in partial fulfillment of the requirements for the degree of

Bachelor of Science

Benjamin Frandsen and Karine Chesnel, Advisors

Department of Physics and Astronomy

Brigham Young University

April 2021

Copyright © 2021 Charlotte Read

All Rights Reserved

## ABSTRACT

Fe<sub>3</sub>O<sub>4</sub> nanoparticles investigated by vibrating sample magnetometry and muon spin relaxation

Charlotte Read

Department of Physics and Astronomy, BYU

Bachelor of Science

Magnetite (Fe<sub>3</sub>O<sub>4</sub>) nanoparticles are responsive in a magnetic field. Three different sizes of Fe<sub>3</sub>O<sub>4</sub> nanoparticles (5 nm, 12.5 nm, and 20 nm) were probed by vibrating sample magnetometry (VSM) and muon spin relaxation ( $\mu$ SR). VSM is a bulk magnetic probe, and  $\mu$ SR is a local magnetic probe. Particles of 5 nm, 12.5 nm, and 20 nm average sizes were found to exhibit strong superparamagnetic characteristics and distinct blocking temperatures. The blocked state transition occurred between 3 K and 45 K for the 5 nm particles, between 80 K and 160 K for 12.5 nm particles, and between 150 K and 300 K for the 20 nm particles. Both the VSM and  $\mu$ SR techniques showed spin-flip energy and magnetic anisotropy.

Keywords: Fe<sub>3</sub>O<sub>4</sub>, magnetite, magnetic nanoparticles, muon spin relaxation, vibrating sample magnetometry, asymmetry

## ACKNOWLEDGEMENTS

I thank Ben Frandsen, Karine Chesnel, and Roger Harrison for their continued support and mentoring. Their belief and encouragement guided not only the course of this research but also the course of my life moving forward. I thank Gerald Morris and the staff of the  $\mu$ SR beamline for hosting me and supporting the Frandsen group's  $\mu$ SR experiment. I thank my friends and family for their support and help in proofreading this thesis. I also thank my parents for instilling in me the confidence that with enough heart and hard work I can do anything I set my mind to.

# Contents

## Table of Contents

v

### 1 Overview

1.1 Magnetic nanoparticles definition.....	6
1.2 Superparamagnetism.....	6
1.3 Vibrating sample magnetometry.....	7
1.4 Muon spin relaxation.....	7
1.5 Brief overview of results.....	8

### 2 Experimental Setup

2.1 Organic synthesis: 5 nm.....	9
2.2 Organic synthesis: 12.5 nm.....	10
2.3 Commercial purchase: 20 nm.....	11
2.4 TEM results.....	11
2.5 VSM conditions.....	13
2.6 $\mu$ SR conditions.....	13

### 3 Results and Conclusions

3.1 TEM and magnetometry results for 5 nm.....	15
3.2 TEM and magnetometry results for 12.5 nm.....	17
3.3 TEM and magnetometry results for 20 nm.....	19
3.4 Interpretation of results.....	20
3.5 Future possibilities.....	22

<b>List of Figures</b>	<b>XXIII</b>
<b>Bibliography</b>	<b>XXV</b>
<b>Index</b>	<b>XXVI</b>

# Chapter 1

## Overview

### 1.1 Magnetic nanoparticles

Magnetic nanoparticles made of  $\text{Fe}_3\text{O}_4$  are responsive in a magnetic field, allowing for unique applications in various technical fields. Because of their variable size, non-toxic nature, and surface chemistry,  $\text{Fe}_3\text{O}_4$  nanoparticles are good options for drug carriers, for contrast agents in magnetic resonance imaging, or for magnetic hyperthermia [1]. Their unique properties come from their small size.  $\text{Fe}_3\text{O}_4$  nanoparticles are ferrimagnetic. If their size is smaller than about 100 nm, they fall in the mono-domain limit, meaning only one ferri-magnetic domain occupies the entire particle. Each individual magnetic domain can be called a nanospin, which results from the individual electronic spins around the iron atoms. The macroscopically observed magnetic properties result from the collective behavior of these nanospins.

### 1.2 Superparamagnetism

At sufficiently high temperatures, magnetic nanoparticles exhibit a superparamagnetic behavior, meaning their nanospins spontaneously fluctuate and flip their direction. The superparamagnetic nature of  $\text{Fe}_3\text{O}_4$  nanoparticles allows the particles to have stronger magnetic fluctuations, which can be useful for certain applications such as magnetic hyperthermia. However, at sufficiently cool temperatures, the flipping stops. Below a specific low temperature state, the nanospins

become progressively immobilized in respect to the observation timing. The temperature where the nanoparticles enter a blocked or immobilized state for a given observation timing is called the blocking temperature. Understanding the blocking transition of  $\text{Fe}_3\text{O}_4$  nanoparticles from the superparamagnetic state to the blocked state is important for establishing the fundamental physics of magnetism on the nanoscale and for understanding the behavior in conditions relevant for technological application. The blocking transition can be explored through a few different methods, two of these being muon spin relaxation and vibrating sample magnetometry.

### **1.3 Muon spin relaxation**

Magnetic nanoparticles have been studied through a variety of techniques, but muon spin relaxation and vibrating sample magnetometry give new insights into their magnetic behaviors. Muon spin relaxation is a specialized technique that is considered a “local probe,” because the individual muons are able to probe the local magnetic field in their immediate vicinity. This provides useful information that often gets averaged out in bulk style probes. The  $\mu\text{SR}$  technique has not seen widespread application to magnetic nanoparticles, although it has played an important role in numerous other magnetic systems. However, the  $\mu\text{SR}$  technique is one of two that will be described in this paper.

### **1.4 Vibrating sample magnetometry**

Vibrating sample magnetometry (VSM) gives additional insight into the particles’ superparamagnetic behavior. Based on the Faraday effect, VSM measures the net magnetization of a material in response to an applied external magnetic field. VSM is a conventional but valuable workhorse technique that is considered a “bulk probe,” meaning it provides

macroscopically averaged information about the magnetic properties. Combining these two techniques gives rich insight into both superparamagnetic behavior and the characteristics of blocking transition.

## **1.5 Brief overview of results**

After studying particles of 5 nm, 12.5 nm, and 20 nm, we were able to extract data on superparamagnetic behavior and blocking transition. As the nanoparticles increased in size, their blocking transition temperature increased substantially. The VSM data taken links the particles' sizes and associated particle distributions to the blocking temperatures. Through  $\mu$ SR data, we see that the blocking transition will vary across a sample of particles with a distribution of sizes. The  $\mu$ SR and VSM results support each other, giving us consistent results about  $\text{Fe}_3\text{O}_4$ 's superparamagnetic behavior and blocking transition temperature.

## Chapter 2

# Experimental Setup

### 2.1 Organic synthesis: 5 nm

$\text{Fe}_3\text{O}_4$  nanoparticles of 5 nm were synthesized through an organic method [3-4]:  $\text{Fe}(\text{acac})_3$  (2 mmol) mixed with phenyl ether (20 mL), hexadecane-1,2-diol (10 mmol), oleic acid (6 mmol), and oleylamine (6 mmol), was heated to approximately 200 °C for 30 minutes, and then was refluxed for 30 min (270 °C). Heating was done under nitrogen. During reflux, aluminum foil was wrapped around the flask to better stabilize the temperature. After the mixture was cooled,



a wash of ethanol-200 proof was added to until the mixture reached a volume by 150%.

Figure 1. Synthesis setup

The set-up for the Altavilla synthesis is shown above.  $\text{Fe}(\text{acac})_3$  (2 mmol) was mixed with phenyl ether (20 mL), hexadecane-1,2-diol (10 mmol), oleic acid (6 mmol), and oleylamine (6 mmol) which was then heated under nitrogen. The aluminum foil helped to insulate and keep the temperature stable during reflux (270 °C).

The mixture was centrifuged approximately 8 minutes at 5000 revolutions per minute; the wash and centrifugation were both performed once more. The organic method left the particles surrounded by a ligand shell made of oleic acid molecules. The process resulted in a dense, black powder of nanoparticles, which were stored in a nitrogen vacuum until use.

## 2.2 Organic synthesis: 12.5 nm

Fe<sub>3</sub>O<sub>4</sub> nanoparticles of 12.5 nm were synthesized through an organic method in two steps [5]. First, Fe(III) Oleate was prepared. We dissolved 5.4 g of FeCl<sub>3</sub>·6H<sub>2</sub>O in 100 mL of methanol. Then, 17 mL of oleic acid was added in 3 equivalent aliquots. A magnetic stirrer was inserted, and the solution was stirred under fast stirring conditions. Then, a NaOH solution of 2.4 g of NaOH in 200 mL of methanol was dropped in at a rate of 1 drop per second. After the NaOH dropped in completely, the stirring rate was decreased but left running for approximately 20 minutes to increase the precipitate yield. This method created a rust-brown color precipitate of ferric oleate which was washed in methanol and left to dry overnight in a nitrogen vacuum. After drying, the precipitate's mass was determined.

The second step involved decomposing the ferric oleate at 300 °C with the solvent octadecene. This was done under nitrogen and left at 300 °C for 30 minutes. The setup was the same as in Fig. 1. except for a larger flask was used. As in the procedure for the 5 nm particles, it was important to watch the temperature of the plastic clips and switch them out about halfway through the 30 minutes. After the mixture was cooled, a wash of methanol was performed. The mixture was centrifuged; the wash and centrifuge were both performed once more. The organic method left the particles surrounded by a ligand shell made of oleic acid molecules. The process resulted in a sticky paste of nanoparticles, which were stored in a nitrogen vacuum until use.

## 2.3 Organic synthesis: 20 nm

Purchased from Cytodiagnostics Inc., the 20 nm particles came in a toluene solution which was evaporated under nitrogen gas. These particles were also surrounded by an oleic acid ligand shell. Evaporation left a dense, dry paste on the bottom of a petri dish which was scraped off with a razor blade.

## 2.4 TEM results

Transmission electron microscopy (TEM) images were taken of the particles to determine average size and size distribution. The images were taken by a ThermoFisher Scientific Tecnai F20 UT at 200 kV. The particles were mixed with either toluene or chloroform to create a solution which was dropped onto a carbon film. This created a monolayer of nanoparticles to be imaged. The mean diameter and standard deviation were measured.

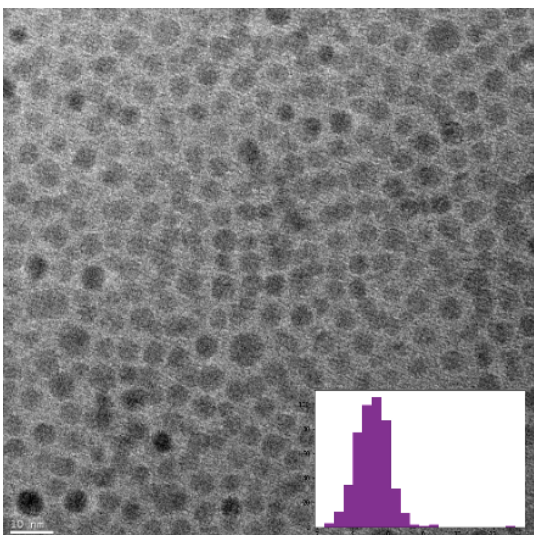
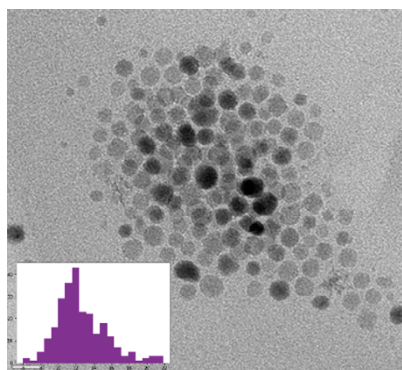


Figure 2. TEM of 5 nm

The Fe<sub>3</sub>O<sub>4</sub> nanoparticles pictured above were synthesized through the Altavilla method [3-4], creating an average size of  $5.16 \pm 0.96$  nm. This particular nanoparticle batch is numbered NP35. Its standard deviation was calculated from a total of 466 imaged nanoparticles. The higher variation in particle size is due to the organic synthesis procedure. Variations in temperature throughout the flask and limited stirring capabilities exposed some particles to higher heat for longer, accentuating the natural size variation. Credit for this TEM image and histogram layover goes to Dr. Karine Chesnel and her graduate student Colby Walker.

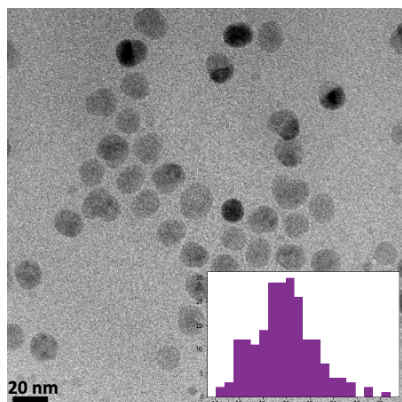
Fig. 2 shows the 5 nm particles in a TEM image. The average size was  $5.16 \pm 0.96$  nm. The standard deviation was calculated from a total of 466 imaged particles. Fig. 6 shows the 12.5 nm particles in a TEM image. The average size was  $12.58 \pm 2.82$  nm. The 20 nm particles were commercially produced and purchased. The average size was  $19.22 \pm 2.37$  nm as seen in Fig. 7. Uneven heating in the organic synthesis procedure may have caused deviation in the particle sizes, but we were still able to get a close-to homogenous size distribution for the 5 nm particles and a slightly less homogenous size distribution for the 12.5 nm particles. The individual particles are surrounded by a ligand shell which is about 1 nm in thickness. These results are consistent with the recent survey done by the Chesnel group on a wider range of  $\text{Fe}_3\text{O}_4$  particle sizes [9].

Figure 3. TEM of 12.5 nm



The  $\text{Fe}_3\text{O}_4$  nanoparticles pictured above were synthesized through the Peng method [5], creating an average size of  $12.58 \pm 2.82$  nm. This particular nanoparticle batch is numbered NP34. The higher variation in particle size is due to the organic synthesis procedure. Variations in temperature throughout the flask and limited stirring capabilities exposed some particles to higher heat for longer, accentuating the natural size variation. Credit for this TEM image and histogram layover goes to Dr. Karine Chesnel and her graduate student Colby Walker

Figure 4. TEM of 20 nm



The  $\text{Fe}_3\text{O}_4$  nanoparticles pictured above were commercially produced and purchased, with an average size of  $19.22 \pm 2.37$  nm. This particular nanoparticle batch is numbered C20. Variations in temperature during synthesis accentuate natural size variation. Credit for this TEM image and histogram layover goes to Dr. Karine Chesnel and her graduate student Colby Walker.

## 2.5 VSM conditions

VSM measurements were taken with a Quantum Design Physical Properties Measurement System (PPMS). This is a thermal-relaxation calorimeter operating with a magnetic field of up to 9 T [6]. The cryogenic sample holder's temperature was set by liquid helium. We filled capsules of with 1 mm<sup>3</sup> of the powdery (5nm and 20 nm) or paste-like (12.5 nm) particles. The nanoparticles were placed in a sample holder and then into the VSM. Under a 10 mT field and with a warming speed of 1 K/min, field cooling (FC) and zero-field cooling (ZFC) measurements were done. The temperature range was 10 K – 400 K. The data collection rate was 1 Hz.

## 2.5 $\mu$ SR conditions

Muon spin relaxation ( $\mu$ SR) data was taken at TRIUMF particle accelerator on the Los Alamos Meson Physics Facility (LAMPF) spectrometer. The  $\mu$ SR technique involves implanting spin-polarized muons one at a time into the sample. Each muon spin undergoes Larmor precession in whatever local magnetic field is present at the muon site, which typically includes the vector sum of any intrinsic magnetic field in the sample as well as an external, applied field. After a muon lifetime of 2.2  $\mu$ s, the muon decays into a positron and two neutrinos, with the positron being emitted preferentially in the direction of the muon spin at the moment of decay. Pairs of detectors are placed around the sample, and the asymmetry or the difference in positron events between the two detectors in the pair can be used to reconstruct the average muon spin direction as a function of time after the muon implantation. This in turn gives insight into the internal magnetic field based on this spin polarization, providing information about the magnetism of the material being studied. The asymmetry data was collected for 9.7  $\mu$ s to give time for the muon's

average lifetime of 2.2  $\mu\text{s}$ . The temperature range was 2 K – 300 K. Fits were done using the program MUSRFIT. The  $\alpha$  parameter was calculated from the fastest recorded relaxation points to get a better zero for asymmetry. Normal calibration using a weak transverse field could not work due to the high magnetic ordering temperatures of  $\text{Fe}_3\text{O}_4$  (Curie temperature around 850 K).

# Chapter 3

## Results and conclusions

### 3.1 TEM and magnetometry results for 5 nm

Much insight into  $\text{Fe}_3\text{O}_4$ 's magnetic properties was gained by examining the VSM results for 5 nm diameter particles. The field cooling (FC) and zero-field cooling (ZFC) measurements are shown below in Fig. 5. The peak in the ZFC line, where it merges with the FC data, shows the blocking transition. When the particles enter this blocked state, their nanospins become progressively immobilized.

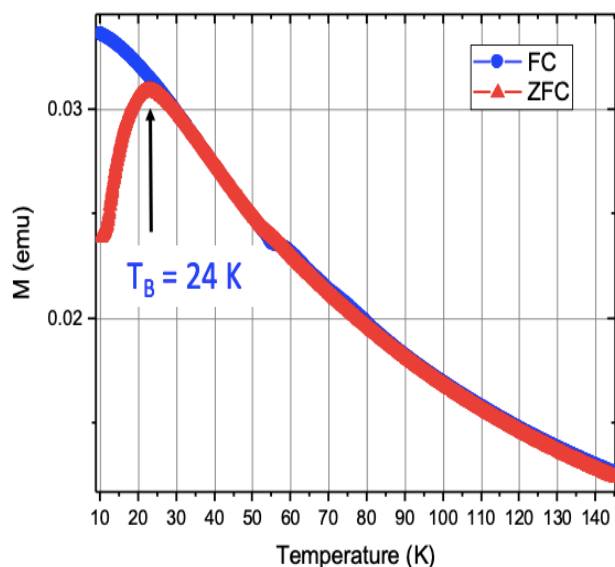


Figure 5. VSM of 5 nm

VSM results for 5 nm particles from NP35. The blocking transition is estimated by ZFC's peak.  $T_B \approx 24$  K. The width of the ZFC peak corresponds with the standard deviation or spread of the nanoparticle sizes (Fig. 2 is included again for emphasis). The blocking transition is a key attribute associated with superparamagnetic behavior. Credit for the VSM image goes to Dr. Karine Chesnel.

In Fig. 5, the blocking temperature is estimated by locating the ZFC's peak:  $T_B \approx 24$  K. The width of the ZFC peak corresponds with the standard deviation or spread of nanoparticle sizes. The VSM results give macroscopically averaged information about the particles' superparamagnetic behavior and blocking transition. The blocking transition is a key attribute associated with superparamagnetic behavior, and the particular blocking temperature found for NP35's 5 nm particles is consistent with other results [7-8].

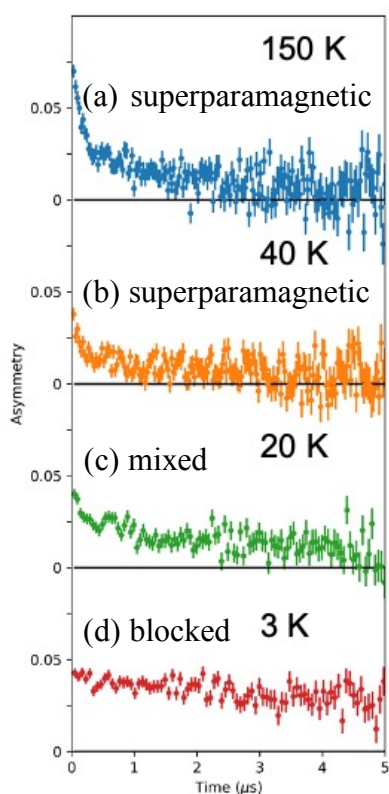


Figure 6. Asymmetry spectra for 5 nm

Asymmetry data for 5 nm particles under zero field indicates superparamagnetic behavior at higher temperatures and a blocking temperature around 30 K. In plots (a) and (b) data points are relaxing down to zero which indicates strongly fluctuating spins and superparamagnetic behavior. However, plot (d) shows finite or flat asymmetry for a long time. This indicates a blocked state with few to none spin fluctuations. Credit for the asymmetry plots goes to Dr. Ben Frandsen.

More insight is given from the  $\mu$ SR characterization. When VSM is considered alongside the  $\mu$ SR technique, both local and bulk information is gathered. Fig. 6 shows representative asymmetry plots under zero field conditions for 5 nm particles. Asymmetry is the difference in positron events between two detectors; this difference is proportional to muon spin polarization which gives the internal magnetic field distribution. In plots (a) and (b) of Fig. 6, the asymmetry decreases down to zero as time evolves, which indicates strongly fluctuating spins and superparamagnetic behavior at  $T > T_B$ . However, plot (d), collected at  $T < T_B$ , shows finite or flat asymmetry for a long time.

The flat asymmetry line in plot (d) indicates a blocked state with few to no spin fluctuations. The asymmetry data in Fig. 6 indicates superparamagnetic behavior at higher temperatures and a blocking temperature approximately 30 K. A strong internal magnetic field is demonstrated by fast relaxation. While asymmetry spectra can be visually inspected to determine the blocking state, spectra can also be integrated in order to identify and characterize the exact transition. In Fig. 7 the asymmetry spectrum is integrated over the first 8  $\mu$ s. The sharp drop from 0 K to about 30 K indicates an increasing number of particles leaving the blocked state. This is a simple way to effectively estimate the blocking transition. The integrated asymmetry plot indicates a blocking transition of 30 K which agrees with the VSM results above [10].

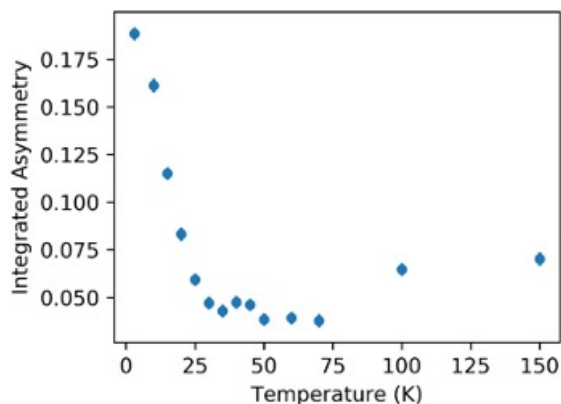


Figure 7. Integrated asymmetry for 5 nm

Integrated asymmetry plot shows asymmetry integrated over the first 8  $\mu$ s for 5 nm particles. The sharp drop from 0 K to about 30 K indicates an increasing number of particles leaving the blocked state. This is a simple way to get effectively estimate the blocking transition of 30 K. Credit for the asymmetry plots goes to Dr. Ben Frandsen.

### 3.2 TEM and magnetometry results for 12.5 nm

These experimental methods provide insight into  $\text{Fe}_3\text{O}_4$  particles with a 12.5 nm diameter. The field cooling (FC) and zero-field cooling (ZFC) measurements are shown below in Fig. 8. The peak in the ZFC line shows when the nanospins become progressively immobilized and the particles enter the blocked state. The blocking transition is estimated by ZFC's peak:  $T_B \approx 160$  K. The width of the ZFC peak corresponds with the standard deviation or spread of nanoparticle sizes which is wider than for the 5 nm particles.

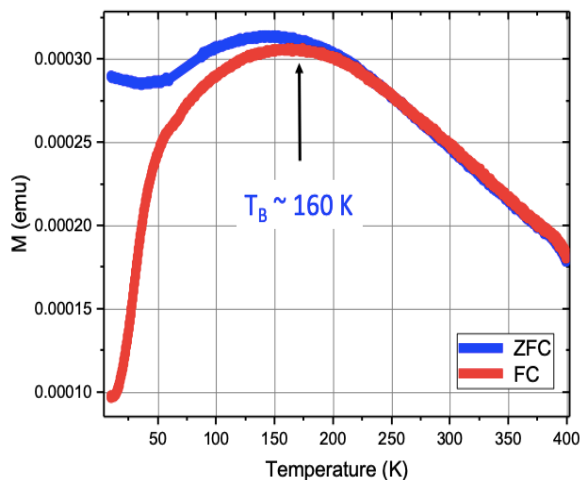


Figure 8. VSM of 12.5 nm

VSM results for 12.5 nm particles from NP34. The blocking transition is estimated by ZFC's peak.  $T_B \approx 160$  K. The width of the ZFC peak corresponds with the standard deviation or spread of the nanoparticle sizes. The blocking transition is a key attribute associated with superparamagnetic behavior. Credit for the VSM image goes to Dr. Karine Chesnel.

In Fig. 9 the asymmetry spectrum is integrated over the first 8  $\mu$ s as described above for the 5 nm particles. The drop in integrated asymmetry indicates a blocking transition of about 80 K. The 12.5 nm data is not as clean due to muons landing in the 1 nm ligand shell. When the muons land in the ligand shell, a combination signal is generated from the nanoparticle and the oleic acid ligand shell. This makes it difficult to isolate the nanoparticle signal and may explain the discrepancy between the blocking temperature observed by  $\mu$ SR and VSM.

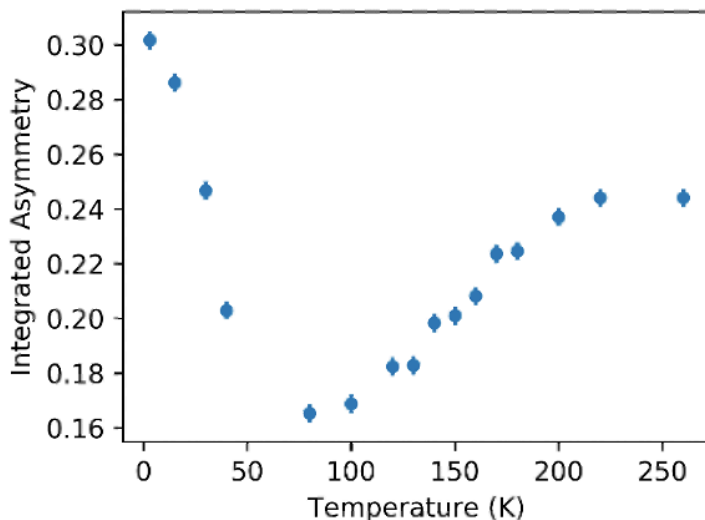


Figure 9. Integrated asymmetry of 12.5 nm

Integrated asymmetry plot shows asymmetry integrated over the first 8  $\mu$ s for 12.5 nm particles. The sharp drop indicates an increasing number of particles leaving the blocked state around 80 K. Credit for the asymmetry plots goes to Dr. Ben Frandsen.

## 3.2 TEM and magnetometry results for 20 nm

These experimental methods provide insight into  $\text{Fe}_3\text{O}_4$  particles with a 20 nm diameter. The field cooling (FC) and zero-field cooling (ZFC) measurements are shown below in Fig. 10.

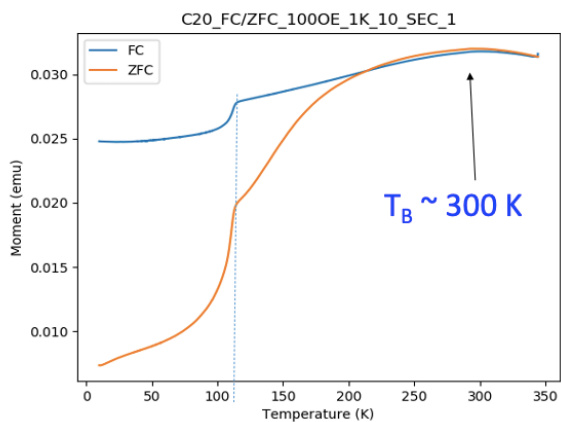


Figure 10. VSM of 20 nm

VSM results for 20 nm particles from C20. The blocking transition is estimated by ZFC's peak.  $T_B \approx 300$  K. The width of the ZFC peak corresponds with the standard deviation or spread of the nanoparticle sizes. The blocking transition is a key attribute associated with superparamagnetic behavior.

Credit for the VSM image goes to Mason Christiansen.

The peak in the ZFC line shows when the nanospins become progressively immobilized and the particles enter the blocked state. The blocking transition is estimated by ZFC's peak:  $T_B \approx 300$  K. The large extent of the ZFC is due to the large spread of nanoparticle sizes as seen in Fig. 10. In Fig. 11 the asymmetry spectrum is integrated over the first 8  $\mu\text{s}$ . The drop in integrated asymmetry indicates blocking transition of about 220 K which is less than but similar to the VSM results above.

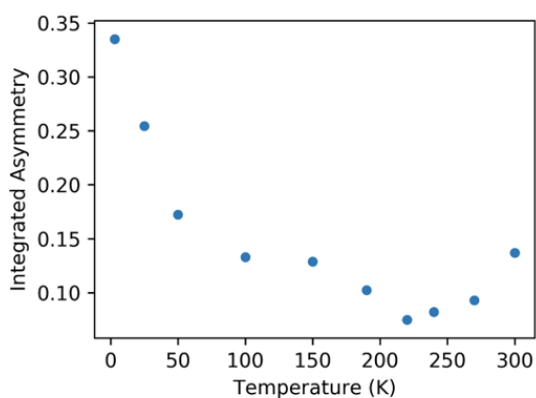


Figure 11. Integrated asymmetry of 20 nm

Integrated asymmetry plot shows asymmetry integrated over the first 8  $\mu\text{s}$  for 20 nm particles. The sharp drop indicates an increasing number of particles leaving the blocked state around 220 K. Credit for the asymmetry plots goes to Dr. Ben Frandsen.

### 3.4 Interpretation of results

By comparing the differing results for 5 nm and 20 nm particles, we can learn even more. The integrated asymmetry gives more accurate local information. From it we see that the blocking transition occurs gradually throughout the sample as the temperature is varied, as opposed to occurring instantaneously in the entire sample at once. This is consistent with the fact that each sample contains a distribution of particle sizes, and we know that particle size is a significant determining factor of the blocking temperature, with larger particles showing higher blocking temperatures. This can be visualized by plotting  $T_B$  as a function of particle diameter, as seen in Fig. 12(a).

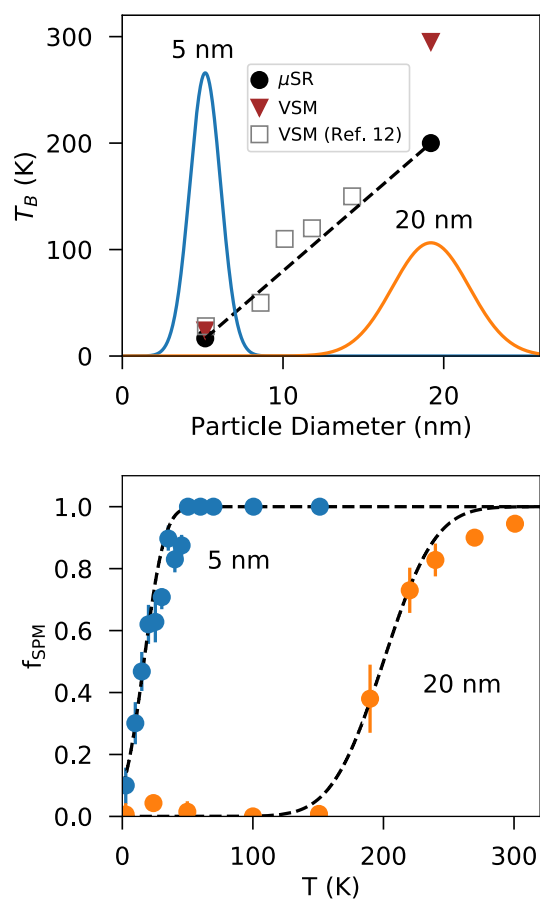


Figure 12.  $T_B$  as a function of particle diameter and Superparamagnetic fraction as a function of temperature

(a) The black dotted line in Fig. 12 shows  $T_B$  as a function of particle diameter. Normalized Gaussian curves are overlaid to show the standard deviation of the 5 nm and 20 nm particles. The standard deviation of the two nanoparticle batches justify the gradual change in blocking transition. Credit for the plots goes to Dr. Ben Frandsen. (b) Calculated superparamagnetic fraction of  $Fe_3O_4$  nanoparticles (dashed curves) compared to experimentally determined results (solid circles) for the 5 nm and 20 nm particles. Experimentally observed values of the superparamagnetic fraction were determined from  $\mu$ SR data fits carried out by other students in the Frandsen research group [10].

The black dotted line in Fig. 12(a) represents a simple linear approximation of  $T_B$  as a function of particle diameter. The equation of the dashed line is  $T_B(D) = AD + B$  where  $D$  is the particle size in nm,  $A = 13$  K/nm, and  $B = -50.8$  K. Normalized Gaussian curves are overlaid to show the standard deviation of the 5 nm and 20 nm particles. The variation of the dashed line across the sample distribution then gives an approximate indication of the range of blocking temperatures that could be expected for a given sample. The standard deviation of the two nanoparticle batches justify the gradual change in blocking transition as seen by the  $\mu$ SR “local probe.” Combining the data from VSM,  $\mu$ SR, and TEM makes possible the inference of  $T_B$  for nanoparticle sizes between what was sampled. In Fig. 12(b), the expected superparamagnetic fraction is calculated based on the slope of the simple linear approximation of  $T_B$  and the width of the Gaussian distributions. This is done by rearranging the linear function  $T_B(D)$  to solve for the cutoff particle size  $D_c(T) = (T - B)/A$ . If we integrate the normalized particle size distribution,  $p(D)$ , up to this cutoff particle size, we are able to determine the expected superparamagnetic fraction for a given temperature. The mathematical equation is represented by

$$f_{SPM}(T) = \int_0^{D_c(T)} p(D) dD.$$

Fig. 12(b) compares this calculated approximation to the experimentally observed values of the superparamagnetic fraction as determined from  $\mu$ SR data fits carried out by other students in the Frandsen research group. Agreement between the calculated and experimental superparamagnetic fractions indicates that the gradual blocking transition is caused by finite particle size distribution. This linear model implies a negative temperature baseline  $B$  and consequently a minimum cutoff size  $D_0 = -\frac{B}{A}$  (around 3.9 nm here) for the blocking transition

to occur. These assumptions are in fact unphysical as one expects nanoparticles of any size to eventually transition into the blocked state or become immobilized at  $T = 0$  K. Consequently, we have been refining this model by a more physical quadratic model which ensures that  $T_B$  remains positive as described in our upcoming paper [10].

### 3.4 Future possibilities

The results from the  $\mu$ SR and VSM data generally agreed, and the results make even more sense when the particle size standard deviation (as determined from the TEM images) is considered. There are many possibilities that could be explored in the future. These experimental methods could be applied to more particle sizes which would provide a more accurate model for  $T_B$  vs. nanoparticle diameter than the simple linear model shown in Fig. 12. Another possibility would be to explore other synthesis methods for  $\text{Fe}_3\text{O}_4$ . The current methods leaves an oleic acid ligand shell which makes it difficult to isolate the signals from just the nanoparticle, especially for the 12.5 nm particles produced by the Peng method [4]. Perhaps a different washing method would leave the particles powdery instead of paste-like. Another possibility would be to compare this data to x-ray scattering data and neutron data since these other two methods would not be as affected by the ligand shell and could provide more information about the structure of the nanoparticles. Additionally, these methods could be applied to other materials besides  $\text{Fe}_3\text{O}_4$ , resulting in even more rich data. The  $\mu$ SR and VSM data results found leave many exciting possibilities for future research in this field.



# List of Figures

## Figure

Figure 1. Synthesis setup.....	9
Figure 2. TEM of 5 nm .....	11
Figure 3. TEM of 12.5 nm.....	12
Figure 4. TEM of 20 nm .....	12
Figure 5. VSM of 5 nm .....	15
Figure 6. Asymmetry spectra for 5 nm .....	16
Figure 7. Integrated asymmetry for 5 nm.....	17
Figure 8. VSM of 12.5 nm .....	17
Figure 9. Integrated asymmetry of 12.5 nm .....	18
Figure 10. VSM of 20 nm .....	19
Figure 11. Integrated asymmetry of 20 nm.....	19
Figure 12. $T_B$ as a function of particle diameter and Superparamagnetic fraction as a function of temperature.....	20

# Bibliography

- [1] Kudr, J., Haddad, Y., Richtera, L., Heger, Z., Cernak, M., Adam, V., & Zitka, O. (2017). Magnetic Nanoparticles: From Design and Synthesis to Real World Applications. *Nanomaterials (Basel, Switzerland)*, 7(9), 243. <https://doi.org/10.3390/nano7090243>
- [3] N. A. Frey, S. Peng, K. Cheng, and S. Sun, *Chem. Soc.Rev.*38, 2532 (2009).
- [4] N. A. Frey, S. Peng, K. Cheng, and S. Sun, *ACS Nano B*, 6081 (2011).
- [5] Nikhil R. Jana, Yongfen Chen, and Xiaogang Peng, *Chemistry of Materials* **2004** 16 (20), 3931-3935, DOI: 10.1021/cm049221k
- [6] J.C. Lashley, M.F. Hundley, et al. *Science Direct*, 43(6) (2003)
- [7] A. Yaouanc and P. D. de R'etotier, *Muon Spin Rotation, Relaxation, and Resonance: Applications to Condensed Matter*, 1st ed. (Oxford University Press, Oxford, 2011).
- [8] K. Chesnel, M. Trevino, Y. Cai, J. M. Hancock, S. J. Smith, and R. G. Harrison, *J. Phys.:* Conf. Ser. 521, 012004 (2014).
- [9] S. Klomp, C. Walker, M. Christiansen, B. Newbold, D. Griner, Y. Cai, P. Minson, J. Farrer, S. Smith, B. J. Campbell, R. G. Harrison, and K. Chesnel, *IEEE T. Magn.* 56, 2300109 (2020).
- [10] Benjamin A. Frandsen, Charlotte Read, Jade Stevens, et al. Submitted to *Phys. Rev. B.* (2021)

# Index

Asymmetry, 13

Blocking temperature, 7, 20

Field cooling, 15

Flipping, 6

Gaussian, 21

Magnetic hyperthermia, 6

Magnetic nanoparticles, 6

Magnetic resonance imaging, 6

Magnetometry, 7

Nanospin, 6

Superparamagnetism, 6

TEM, 11

Zero-field cooling, 15